MNRAS 000, 1–21 (2020) Preprint 19 May 2020 Compiled using MNRAS LATEX style file v3.0

Diffusion of large-scale magnetic fields by reconnection in MHD turbulence

R. Santos-Lima,[1⋆] G. Guerrero,[2†] E. M. de Gouveia Dal Pino,[1‡] A. Lazarian[3,4§]
[1] *Instituto de Astronomia, Geofísica e Ciências Atmosféricas, Universidade de São Paulo, R. do Matão, 1226, São Paulo, SP 05508-090, Brazil*
[2] *Physics Department, Universidade Federal de Minas Gerais, Av. Antonio Carlos, 6627, Belo Horizonte, MG, Brazil, 31270-901*
[3] *Department of Astronomy, University of Wisconsin, 475 North Charter Street, Madison, WI 53706, USA*
[4] *Center for Computation Astrophysics, Flatiron Institute, 162 5th Ave, New York, NY 10010*

Last updated 2015 May 22; in original form 2013 September 5

ArXiv:2005.07775, 15 May 2020

Miljenko Čemeljić, SHAO Visiting Scientist (PIFI)

Outline

- Introduction to reconnection
- MHD turbulence
- Turbulent reconnection
- Reconnection diffusion
- Historic lesson: Onsager (1940-ies) on “ideal turbulence”
- Takeaway points

Introduction to reconnection

-The first mentioning of reconnection: in the solar physics context by Giovanelli (1946). He considered chromospheric solar flares as a phenomenon arising from a slow build-up of energy stored in the magnetic field, which is then suddenly released into thermal and kinetic energy. There is still no definitive description, but there are (too) many developments (=papers).

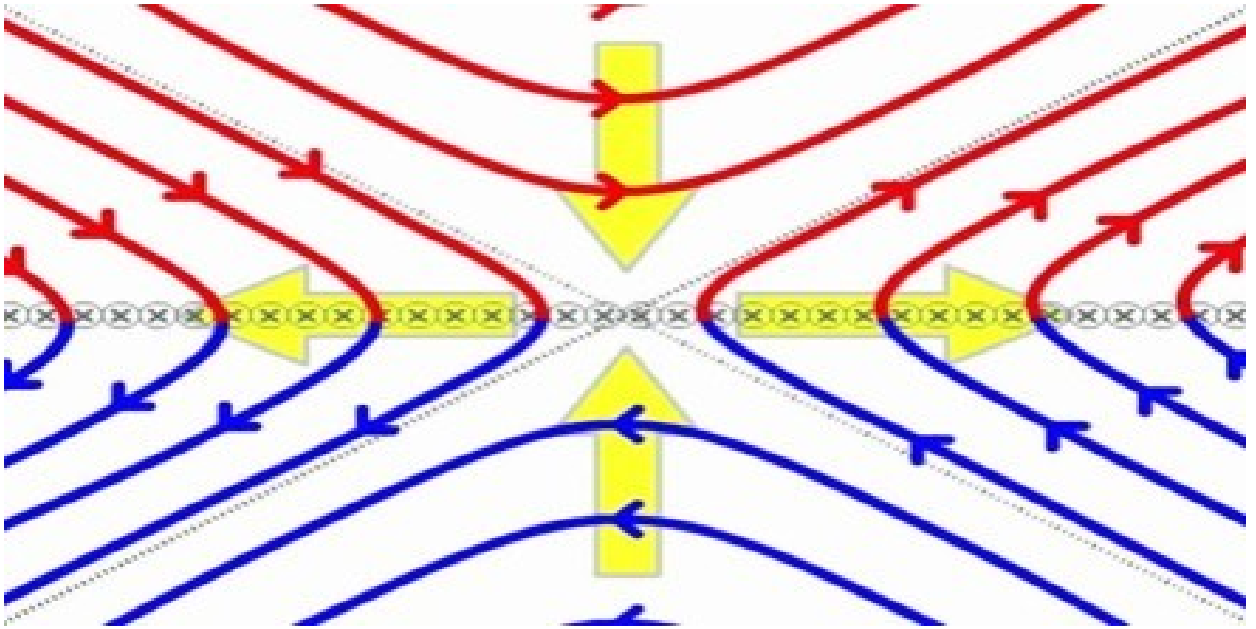

What is re-connecting?

Magnetic field lines, when they have time to do it before the fluid moves them away from each other. In the ideal MHD approximation, the Reynolds magnetic number $R_m=VL/\eta >>1$, there is no reconnection, magnetic field is "frozen in" in the fluid. [note: the Lundquist number $R_L=S$ is equal to R_m with $V=V_{Alfven}$]. But, what happens when the lines are twisted? Does the topology of the lines change? Our understanding of the cosmic magnetic field depends on the answer, e.g. contemporary dynamo theories rely on the positive answer. Further discussion is based on this assumption.

“Classical” reconnection

-Sweet-Parker (1958,1957):

larger length L=>slower reconnection, Vrec=($V_A \eta/L$)^½

-too slow to describe observations $=V_A/\sqrt{S}$

-obtained in simulations (Biskamp et al.).

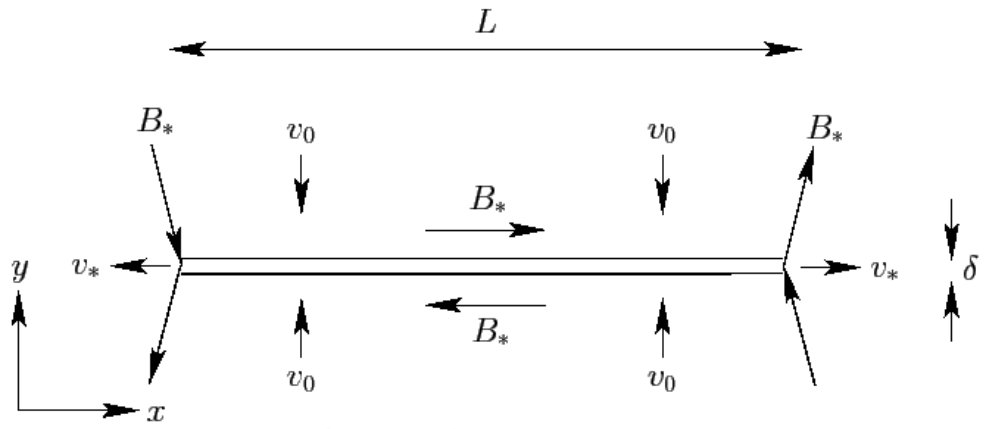

Figure 26: *The Sweet-Parker magnetic reconnection scenario.*

-Petschek (1964): Vrec=V_A/ln(S)

shorter length L ~ d =>faster reconnection

-controversial; never obtained in simulations without enhanced resistivity.

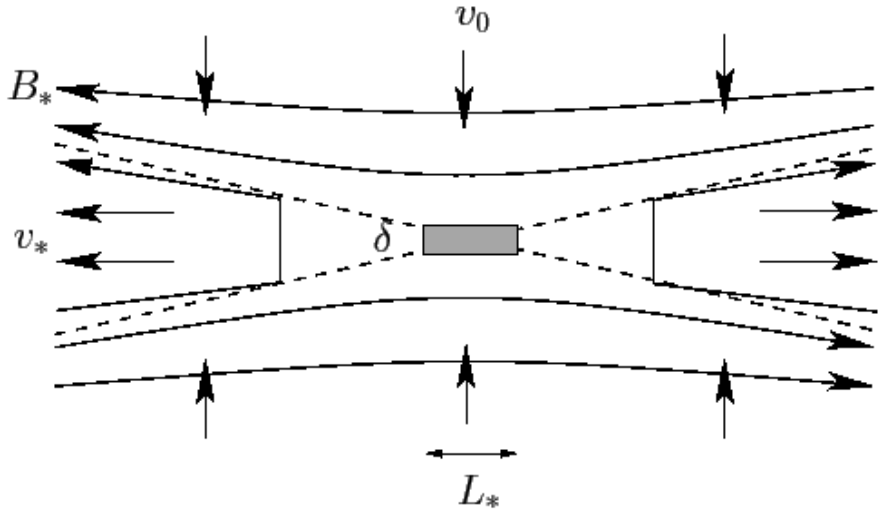

Figure 27: *The Petschek magnetic reconnection scenario.*

Reconnection rate in the two-dimensional case can be estimated in the different ways, depending on the dominating physical properties in the system. The first such estimate was given by Parker,[14,15] with the Alfvén Mach number $M_{SP} = V_i/V_A = S^{-1/2}$. The Lundquist number $S = \tau_{Ohm}/\tau_{adv} = LV_A/\eta$ is the ratio of the advective over the resistive term in the Eq. (3). In an astrophysical case, the length scale is so large that the obtained reconnection rate is way too small, when compared to the observed reconnection events on the Sun or in the Earth's magnetosphere.

To improve the model, Petschek[17] assumed that the plasma can also be accelerated by slow shocks. Then, the reconnection rate is $M_P = \pi/(8 \ln S)$. For the current sheet in a small region, the Petschek model gives orders of magnitude faster reconnection than the Sweet-Parker model, up to 0.1. The reason is that in the Petschek model the reconnection rate is not strongly dependent on the Lundquist number. For the current sheet extending to the whole reconnection area, both models give the same reconnection rate.

The reconnection rate can also be estimated from the turbulent motions.[10] For the case of only Ohmic resistivity, we can estimate the distance to which a magnetic field can diffuse in time τ_D as $\ell \sim (\eta\tau_D)^{1/2}$. This means that two lines can merge only if their distance is of the order of $\Delta = \ell/\sqrt{S}$. In combination with mass conservation, one obtains the reconnection rate M_{SP}.

(**from Čemeljić & Huang, 2014**; Eq. 3 Is induction eq. $\frac{\partial \boldsymbol{B}}{\partial t} - \nabla \times \left(\boldsymbol{V} \times \boldsymbol{B} - \frac{4\pi}{c} \eta \boldsymbol{j} \right) = 0$

We confirmed that in 3D, reconnection rate increases by a factor √2).

Spitzer resistivity

Spitzer[1] showed that to obtain an accurate theoretical value of classical resistivity two effects have to be taken into account. First of all, the electron distribution function gets distorted from a simple shifted Maxwellian because electrons with larger velocities experience fewer collisions with ions, as the Coulomb collision frequency is inversely proportional to the third power of velocity ($\nu_{ei} \sim 1/v^3$), and are thus accelerated more. Secondly, electron-electron collisions provide friction drag on the high velocity tail of the distribution function, leading to its Maxwellization. After incorporating these effects, the resistivity $\eta_\parallel$ along the magnetic field or in the unmagnetized plasma can be represented in the form:[2]

$$\eta_\parallel^{\text{Spitzer}} = \frac{\sqrt{2m_e}Z_{\text{eff}}e^2 \ln \Lambda}{12\pi^{3/2}\epsilon_0^2 T_e^{3/2}} \times F(Z_{\text{eff}}), \tag{1}$$

where T_e is the electron temperature, Z_{eff} is the effective ionic charge, $\ln \Lambda = \ln(T_e^{3/2}/\sqrt{\pi Z e^3 n^{1/2}})$ is the Coulomb logarithm, and $F(Z_{\text{eff}})$ is approximated by:

$$F(Z) \simeq \frac{1 + 1.198Z + 0.222Z^2}{1 + 2.966Z + 0.753Z^2}. \tag{2}$$

Thus, in the important case of Z_{eff} equal to 1,

$$\eta_\parallel^{\text{Spitzer}}[\text{Ohm} \times \text{m}] = 0.53 \times 10^{-4} \frac{\ln \Lambda}{T_e^{3/2}[\text{eV}]}. \tag{3}$$

Since binary collisions leading to a large angle scattering are neglected in the Spitzer calculation, the final result has the uncertainty of $1/\ln \Lambda$.[4]

The main assumptions of the unmagnetized Spitzer calculation are the following: (1) steady-state, (2) energy gained by an electron due to acceleration in the electric field between collisions is negligible compared to the electron thermal energy ($eE\lambda_{\text{mfp}} \ll kT$), which means that the electron distribution function does not strongly deviate from Maxwellian, and (3) plasma is completely ionized, so collisions with neutrals are negligible.

Spitzer also demonstrated that for the case when a strong uniform magnetic field ($\rho_e \ll \lambda_{\text{mfp}}$) is applied perpendicular to the direction of electric field and plasma current, the cross-field or transverse resistivity is approximately twice as large as the parallel resistivity for $Z_{\text{eff}}=1$:

$$\eta_\perp^{\text{Spitzer}} = 1.96 \times \eta_\parallel^{\text{Spitzer}}. \tag{4}$$

For larger Z_{eff} the ratio $\eta_\perp / \eta_\parallel$ increases (see Table 1 of Ref.

Turbulent reconnection

-Both Sweet-Parker and Petchek models use the normal, Spitzer resistivity and result in reconnection rates much below what is observed. In the actual solar flare or other astronomical case, the resistivity could be greatly enhanced, leading to a much faster energy release.

We can divide schemes for fast reconnection into those that **a)** alter the microscopic resistivity, broadening the current sheet by some physical process, and **b)** those that change global geometry of the model, reducing the boundary layer length Lx (the 1st example being Petchek's model). In a mixed approach, Lazarian & Vishniac (1999) introduced the concept of turbulent reconnection.

THE ASTROPHYSICAL JOURNAL, 517:700–718, 1999 June 1

RECONNECTION IN A WEAKLY STOCHASTIC FIELD

A. LAZARIAN[1,2] AND ETHAN T. VISHNIAC[3]

Received 1998 October 28; accepted 1999 January 10

ABSTRACT

We examine the effect of weak, small-scale magnetic field structure on the rate of reconnection in a strongly magnetized plasma. This affects the rate of reconnection by reducing the transverse scale for reconnection flows and by allowing many independent flux reconnection events to occur simultaneously. Allowing only for the first effect and using Goldreich & Sridhar's model of strong turbulence in a magnetized plasma with negligible intermittency, we find a lower limit for the reconnection speed $\sim V_A \mathscr{R}_L^{-3/16} \mathscr{M}^{3/4}$, where V_A is the Alfvén speed, $\mathscr{R}_L$ is the Lundquist number, and $\mathscr{M}$ is the large-scale magnetic Mach number of the turbulence. We derive an upper limit of $\sim V_A \mathscr{M}^2$ by invoking both effects. We argue that generic reconnection in turbulent plasmas will normally occur at close to this upper limit. The fraction of magnetic energy that goes directly into electron heating scales as $\mathscr{R}_L^{-2/5} \mathscr{M}^{8/5}$, and the thickness of the current sheet scales as $\mathscr{R}_L^{-3/5} \mathscr{M}^{-2/5}$. A significant fraction of the magnetic energy goes into high-frequency Alfvén waves. The angle between adjacent field lines on the same side of the reconnection layer is $\sim \mathscr{R}_L^{-1/5} \mathscr{M}^{6/5}$ on the scale of the current sheet thickness. We claim that the qualitative sense of these conclusions, that reconnection is fast even though current sheets are narrow, is almost independent of the local physics of reconnection and the nature of the turbulent cascade. As the consequence of this the Galactic and solar dynamos are generically fast, i.e., do not depend on the plasma resistivity.

Subject headings: galaxies: magnetic fields — MHD

Turbulent reconnection

-The geometry of the model is changed in LV99- turbulence sets the scale:

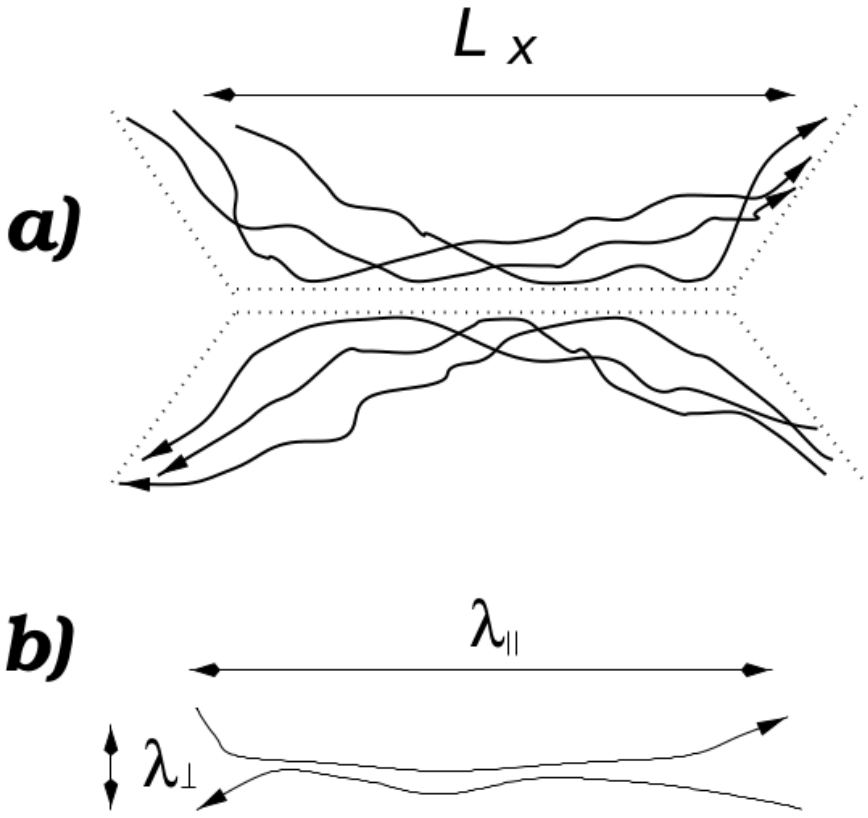

FIG. 2.—(*a*) Structure of the reconnection region when the field is turbulent. Local reconnection events happen on the small-scale $\lambda_{\parallel}$ rather than L_x and this accelerates reconnection. The plasma is redistributed along the field lines in a layer of thickness $\langle y^2 \rangle^{1/2}$, which is much thicker than the region $\sim \lambda_{\perp}$ from which the ejection of the magnetic field takes place. (*b*) Local structure of magnetic field lines.

In the presence of a stochastic field component, magnetic reconnection dissipates field lines not over their entire length $\sim L_x$ but only over a scale $\lambda_{\parallel} \ll L_x$ (see Fig. 2*b*), which is the scale over which the magnetic field line deviates from its original direction by the thickness of the Ohmic diffusion layer $\lambda_{\perp}^{-1} \approx \eta / V_{\rm rec,local}$. If the angle ϕ of field deviation does not depend on the scale, the local reconnection velocity would be $\sim V_{\rm A} \phi$ and would not depend on resistivity. We claim in § 3 that ϕ does depend on scale. Therefore, the *local* reconnection rate $V_{\rm rec,local}$ is given by the usual Sweet-Parker formulae but with $\lambda_{\parallel}$ instead of L_x, i.e., $V_{\rm rec,local} \approx V_{\rm A}(V_{\rm A} \lambda_{\parallel}/\eta)^{-1/2}$. It is obvious from Figure 2*a* that $\sim L_x/\lambda_{\parallel}$ magnetic field lines will undergo reconnection simultaneously (compared with a one-by-one line reconnection process for the Sweet-Parker scheme). Therefore, the overall reconnection rate may be as large as $V_{\rm rec,global} \approx V_{\rm A}(L_x/\lambda_{\parallel})(V_{\rm A} \lambda_{\parallel}/\eta)^{-1/2}$, which means that the reconnection efficiency critically depends on the value of $\lambda_{\parallel}$. More realistically, we will find that there are other global constraints that end up determining the actual global reconnection speed.

The relevant values of $\lambda_{\parallel}$ and $\langle y^2 \rangle^{1/2}$ depend critically on the magnetic field statistics. Therefore, in the next section we will briefly explore the expected properties of magnetic turbulence.

Magnetic turbulence

-First simple model of incompressible MHD turbulence was proposed independently by Iroshnikov (1963) and Kraichnan (1965) based on the interactions of triads of waves.

Triads of waves:

-A good explanation of the principal of nonlinear wave-wave interactions is provided by Holthuijsen[ref.14 in Simon P. Neill, M. Reza Hashemi, "Fundamentals of Ocean Renewable Energy", 2018]: **Two wave paddles, generating waves of different frequencies and directions, are placed in two corners along one side of a tank of constant water depth.** The resulting waves create a diamond pattern of crests and troughs, which has its own wave length, speed, and direction. This diamond pattern would interact with a third-wave component, if this third wave had the same wave length, speed, and direction as the diamond pattern. This is the triad wave-wave interaction, which redistributes wave energy within the spectrum due to resonance. Although each of the individual wave components can gain or lose energy, the sum of the energy at each point in the tank would remain constant. In deep water, it is not possible to meet these resonant conditions (i.e. matching of wave speed, length, and direction), and so triad wave-wave interactions cannot occur in deep water. However, in deep water it is possible for a pair of wave components to interact with another pair of wave components in a quadruplet wave-wave interaction.

Quadruplets transfer wave energy in deep water from the peak frequency to lower frequencies, whereas triads transfer energy from lower to higher frequencies, and transform single-peaked spectra into multiple-peaked spectra as they approach the shore. Both are included as source terms in third-generation wave models, and it is noted that both are computationally expensive. Triads, in particular, are often omitted in wave model simulations, whereas quadruplets are often included.

Magnetic turbulence

Sridhar & Goldreich (1995, 1995,1997) criticized Iroshnikov-Kraichnan, in which they obtained the energy transfer rate as:

$$\tau_{nl}^{-1} \approx \frac{(kv_k)^2}{\omega_A}, \tag{A1}$$

where k is the magnitude of a wavevector, v_k is the rms fluid velocity contributed from power on the scale k^{-1}, $\omega_A \equiv k_\parallel V_A$ is the Alfvén wave frequency, $k_\parallel$ is the wavevector component parallel to the magnetic field direction, and V_A is the Alfvén velocity. In the original picture the power was assumed to spread isotropically in wavevector space. As long as $v_k < V_A$ this

arguing that the diffusion of power toward larger values of $k_\parallel$ is strongly suppressed.

This claim, that three wave interactions are completely suppressed has been strongly criticized (Montgomery & Matthaeus 1995 ; Ng & Bhattacharjee 1996), but in Goldreich & Sridhar (1997) it was shown convincingly that the effect of residual three wave couplings is consistent with a picture in which the basic nonlinear timescale is set by equation (A1), but with an anisotropic spectrum in which virtually all of the transfer of power between modes moves energy toward larger $k_\perp$ while leaving $k_\parallel$ unchanged.

They proposed calling this regime “intermediate turbulence” since while the nonlinear decay rate is identical to the usual expression for weak turbulence among dispersive waves, in this case the higher order mode couplings are all comparably important. Lazarian and Vishniac approach is based on this model.

Magnetic turbulence

If we invoke the constancy of the local energy through the cascade as a function of scale, then from equation (A1) we see that in this regime

$$v_k \propto k_\perp^{-1/2} , \tag{A2}$$

where we have assumed that $k_\perp \gg k_\parallel$.

As the power cascades to larger values of $k_\perp$ the magnetic field becomes progressively less important in the mode dynamics. Eventually we have

$$k_\parallel V_A \leq k v_k . \tag{A3}$$

In this limit the motions are no longer wavelike, the magnetic field exerts only a weak influence on the dynamics, and the fluid motions resemble ordinary hydrodynamical turbulence with a nonlinear timescale $\sim k v_k$. Since $k_\parallel$ is no longer privileged, the cascade of power is in the direction of increasing isotropy. Since $k_\perp \gg k_\parallel$ this implies an increase in $k_\parallel$.

If energy is injected on some scale l, with $v_l \leq V_A$, then we expect the cascade to transfer energy to larger $k_\perp$ until the condition expressed in equation (A3) is satisfied. At this point the turbulence is no longer wavelike (since $\tau_{nl}^{-1} \sim k_\parallel V_A$). However, since turbulence tends toward isotropy when the magnetic field is completely negligible, we expect $k_\parallel$ and $k_\perp$ to increase in tandem so that equation (A3) is just marginally satisfied. This is the regime of strong turbulence described in GS95. At all smaller parallel wavelengths fluid motions bend magnetic field lines easily. Consequently, we expect most of the power in energy spectrum to be centered around wavenumbers such that

$$k_\parallel \sim k_\perp \frac{v_k}{V_A} . \tag{A4}$$

We approximate the energy transfer rate for the turbulent cascade, $\dot{\mathscr{E}}$, for $v_l \leq V_A$ as

$$\dot{\mathscr{E}} \approx \frac{v_l^4}{l V_A} , \tag{A5}$$

if $v_l \leq V_A$ on the scale l. The usual hydrodynamic choice $\dot{\mathscr{E}} \approx (v_l^3/l)$ is valid otherwise, although not relevant for our present discussion. When the magnetic field is weak and the largest scales in the turbulent cascade are essentially hydrodynamic then we can identify l with the scale of equipartition so that $v_l^2 \sim V_A^2$.

This kind of hand-waving arguments are extensively used, but LV99 claim and show, using different models that: “the qualitative nature of our results, that a weak stochastic component to the field structure can have a dramatic effect on reconnection rates, is not sensitive to the details of the model we adopt”.

Magnetic turbulence, equations

If energy is injected on some scale l, with $v_l \leq V_A$, then GS95 predict that

$$k_\parallel \approx l^{-1}(k_\perp l)^{2/3}\left(\frac{v_l}{V_A}\right)^{4/3}, \quad (1)$$

$$\tau_{nl}^{-1} \approx \frac{v_l}{l}(k_\perp l)^{2/3}\left(\frac{v_l}{V_A}\right)^{1/3}, \quad (2)$$

while the rms fluid velocity is given by

$$v_k \approx v_l(k_\perp l)^{-1/3}\left(\frac{v_l}{V_A}\right)^{1/3}. \quad (3)$$

$$\frac{d\langle y^2\rangle}{dx} \sim \frac{\langle y^2\rangle}{\lambda_\parallel}, \quad (4)$$

where $\lambda_\parallel^{-1} \approx k_\parallel$, $k_\parallel$ is the parallel wavevector chosen so that the corresponding vertical wavelength, $k_\perp(k_\perp)$, is $\sim\langle y^2\rangle^{1/2}$ and x is the distance along an axis parallel to the mean magnetic field. Therefore, using equation (1) one gets

$$\frac{d\langle y^2\rangle}{dx} \sim l\left(\frac{\langle y^2\rangle}{l^2}\right)^{2/3}\left(\frac{v_l}{V_A}\right)^{4/3}, \quad (5)$$

where we have substituted $\langle y^2\rangle^{-1/2}$ for $k_\perp$. This expression for the diffusion coefficient will only apply when y is small enough for us to use the strong turbulence scaling relations, or in other words when $\langle y^2\rangle < l^2(v_l/V_A)^4$. Larger bundles will diffuse at a maximum rate of $l(v_l/V_A)^4$. For small $\langle y^2\rangle$ equation (5) implies that a given field line will wander perpendicular to the mean field line direction by an average amount

$$\langle y^2\rangle^{1/2} = \frac{(3x)^{3/2}}{l^{1/2}}\left(\frac{v_l}{V_A}\right)^2 \quad (6)$$

in a distance x. The fact that the rms perpendicular displacement grows faster than x is significant. It implies that if we consider a reconnection zone, a given magnetic flux element that wanders out of the zone has only a small probability of wandering back into it.

Turbulent reconnection

4.1. *Constraints on Reconnection Rate*

Outflow of matter from the reconnection layer constrains the achievable reconnection rates. In the presence of turbulence the thickness of the outflow layer increases with L_x according to equation (6):

$$\langle y^2 \rangle^{1/2} \sim L_x \left(\frac{L_x}{l}\right)^{1/2} \left(\frac{v_l}{V_A}\right)^2 , \qquad (7)$$

when $l > L_x$ and

$$\langle y^2 \rangle^{1/2} \sim (L_x l)^{1/2} \left(\frac{v_l}{V_A}\right)^2 , \qquad (8)$$

when $L_x > l$. Therefore, the upper limit on V_{rec} imposed by large-scale field line diffusion is

$$V_{rec} < V_A \min \left[\left(\frac{L_x}{l}\right)^{1/2} , \left(\frac{l}{L_x}\right)^{1/2} \right] \left(\frac{v_l}{V_A}\right)^2 . \qquad (9)$$

This limit on the reconnection speed is fast, both in the sense that it does not depend on the resistivity and in the sense that it represents a large fraction of the Alfven speed. **Eq. 9 is not only an upper limit on the global reconnection speed but often a reasonable estimate for its actual value.**

Turbulent reconnection

The minimal estimate of V_{rec} given in the previous subsection is based on the assumption that reconnection proceeds sequentially, that is, the reconnection speed is simply the speed with which reconnection propagates through a single flux element. This is not obviously correct, since the reconnection zone contains many independent reconnection events at any one time. We need to define a global reconnection speed, V_{rg}, which describes the rate at which flux is reconnected throughout the reconnection zone.

In order to arrive at a reasonable estimate of this speed, we have to determine which aspect of reconnection sets a limit on its efficiency. There are four possibilities:
-the mass flow from the reconnection zone itself
-the speed with which reconnected flux elements move across the reconnection zone and of the edge
-the ejection of the flux associated with the shared magnetic field component,
-the mass flow from the contact volume (roughly everything within a distance L of the reconnection zone).

In the case of Sweet-Parker reconnection, the first process provides the critical constraint (and the third and fourth are not separate constraints).

Turbulent reconnection

Final conclusions of the LV turbulent reconnection:

- The rate of magnetic reconnection is increased dramatically in the presence of a stochastic component to the magnetic field. This component arises naturally whenever turbulence is present. Even when the turbulent cascade is weak the resulting reconnection speed is independent of the Ohmic resistivity.

-The second parameter in determining the reconnection speed is not some aspect of the microphysics, but the level of field stochasticity (or the large-scale kinetic energy feeding the turbulent cascade). As reconnection proceeds the local turbulent cascade will grow stronger and the initial level of stochasticity will matter less and less. On the contrary, microphysical processes widely believed to speed up reconnection, i.e., anomalous resistivity, fail in interstellar conditions.

-There exists a minimal reconnection speed, $V_r = V_A S^{(-3/16)}$, much faster than the Sweet-Parker estimate, but still unrealistically slow.

Reconnection diffusion

Now to the article which I am reviewing.

Authors consider as a proven fact that turbulence in astrophysical media induces fast magnetic reconnection, which consequently leads to large-scale magnetic flux diffusion at a rate independent of the plasma micro-physics. The concept is still debated, but they argue that there is substantial body of positive theoretical results and numerical tests in Kowal, et al. (2009, 2017, 2020) – a thorough review is given in the book by Lazarian (2020).

Highlight from the abstract:
-for the first time are shown simulations of compressible MHD turbulence with the suppression of the cascade in the direction parallel to the mean magnetic field, which is consistent with incompressible weak turbulence theory.

-authors also verified that the energy cascading time in their simulations does not follow the scaling with Alfven Mach number predicted for the weak turbulence regime, in contradiction with the RD theory assumption.

Reconnection diffusion

The process of changing of magnetic field topology in turbulent fluid is different in turbulent versus laminar fluid. The motions in the ionized gas in turbulent gas produce tangling and wandering of the magnetic field lines which give origin to several micro-sites of magnetic reconnection. This process is independent on how small is the Ohmic resistivity which is always present in any real plasma. Reconnection micro-sites are continuously formed and spread all over the turbulent plasma volume, so that the field lines topology can be modified, and large-scale magnetic flux can be transported through the gas.

Such a result implies that the flux freezing concept is seriously altered.

The speed at which the magnetic flux is transported in such conditions is independent of the electric resistivity of the plasma, or the degree of its ionization but is regulated by the turbulence parameters.

Reconnection diffusion

The concept of standard turbulent mixing described in LV99 is based on the idea that the field lines are mixed passively by the turbulent eddies, without taking into account the effects of the magnetic field on the turbulent cascade.

The concept of magnetic diffusion via turbulent reconnection —Reconnection Diffusion (RD) covers the interesting situation in which the magnetic forces are dynamically important (e.g. in the late stages of star formation). It relies on the fact that the fast reconnection induced by the MHD turbulence is independent of the value of the electric resistivity in the plasma. It is also not altered by the effects of ambipolar drift on the scales where turbulence exists.

RD predicts that the diffusion coefficient η_{RD} for large-scale magnetic fluxes (i.e., scales larger than the injection or forcing scale of the turbulence) depends on the turbulence parameters. In the case of super-Alfvénic turbulence, when the Alfvénic Mach number, $M_A = U_{turb} / V_A$ (where Uturb is the turbulent velocity and V_A is the local Alfvén velocity) is larger than one, it coincides with the standard turbulent mixing coefficient, $\eta_{RD} \sim L_{turb} U_{turb}$, (the length and the velocity of the turbulence at the injection scale, respectively). On the other hand, in the regime of sub-Alfvénic turbulence ($M_A < 1$), this value is reduced by a factor proportional to the third power of M_A: $\eta_{RD} \sim L_{turb} U_{turb} M_A^3$

Therefore, according to the RD theory, the efficiency of the magnetic flux transport strongly depends on the local turbulence regime.

Reconnection diffusion

In previous work they investigated numerically the removal of magnetic flux from collapsing turbulent molecular clouds and protostellar disks, considering an “ideal” MHD approach (i.e., the microscopic magnetic dissipation term was not considered explicitly in the induction equation, although an effective value is always present due to the numerical discretization of the equations). They found that the magnetic flux removal by RD is efficient in these systems, and helps the gravitational collapse of the structures.

Previous works focused mostly on the super and trans-Alfvénic regimes of the turbulence where the reconnection diffusion coefficient is controlled by $\eta_{RD} \sim$ Lturb Uturb. The aim of this work is to test quantitatively the prediction of the second equation, $\eta_{RD} \sim$ Lturb Uturb M_A^3, by using 3D MHD simulations.

It is also the first attempt to generate simulations of stationary weak MHD turbulence (the cenario invoked by the RD theory) in the presence of finite compressibility, which is more realistic for astrophysical environments.

Reconnection diffusion

In situations where the energy cascading time at the injection scale is larger than the molecular or numerical viscous time (implying a low effective Reynold's number), the decorrelation time of the velocity, $\tau_{\rm dec}$, can be more closely related to the dissipation time, $\tau_{\rm diss} \sim \ell^2/\nu$, where ν is the molecular viscosity. The magnetic field diffusion driven by turbulence in this case will depend on the microscopic diffusion and, if $\tau_{\rm dec} \sim \tau_{\rm diss}$, then the diffusivity becomes dependent on the molecular viscosity, ν.

In our discussion we considered only one component of MHD turbulence, namely, Alfvén modes and disregarded the slow and fast modes (see Cho & Lazarian 2003). This is due to the fact that Alfvén modes are the most important in mixing the medium.

used the PENCIL CODE [2] for numerically solving the set of compressible, isothermal, MHD equations:

$$\frac{D\ln\rho}{Dt} = -\nabla\cdot\mathbf{u}, \tag{8}$$

$$\frac{D\mathbf{u}}{Dt} = -c_s^2\nabla\ln\rho + \frac{1}{\rho}\mathbf{J}\times(\mathbf{B_0}+\mathbf{B}) + \nu_3\nabla^6\mathbf{u} + \mathbf{f}, \tag{9}$$

$$\frac{\partial\mathbf{A}}{\partial t} = \mathbf{u}\times(\mathbf{B_0}+\mathbf{B}) + \eta_3\nabla^6\mathbf{A}, \tag{10}$$

where $D/Dt = \partial/\partial t + \mathbf{u}\cdot\nabla$ is the lagrangian derivative, $\mathbf{A}$ is the magnetic potential vector, $\mathbf{B} = \nabla\times\mathbf{A}$ is the magnetic field generated by the internal currents, $\mathbf{J} = \nabla\times\mathbf{B}/\mu_0$ is the current density, μ_0 is the magnetic permeability, ν_3 and η_3 are, respectively, the coefficients of hyper-viscosity and magnetic hyper-diffusivity, c_s is the isothermal sound speed, $\mathbf{u}$ is the velocity, ρ is the density, and $\mathbf{f}$ represents the force responsible for the turbulence injection. We use the hyper-viscosity and magnetic hyper-diffusivity schemes with the aim of obtaining a turbulent spectra with an extension as large as possible for each considered resolution (Borue & Orszag 1995; Haugen & Brandenburg 2004). The value of the coefficients were minimized such that numerical stability is guaranteed.

Reconnection diffusion

Table 1. Runs parameters

runs set	$L_\parallel$x$L_\perp$	res.	v_0/c_s	$v_0/v_{A,0}$	v_{rms}/v_0	forcing	$k_\parallel L/2\pi$	$k_\perp L/2\pi$	$[\tilde{t}_0, \tilde{t}_1]$[a]	$\tilde{\nu}_3$, $\tilde{\eta}_3$[b]
16L-Ms0.32-A	16Lx1L	$2048, 128^2$	0.32	0.8, 0.57, 0.4, 0.2 0.1	1.10, 1.18, 1.18, 1.22 1.33	A	[0, 4]	[3, 4]	[3, 8]	2.1×10^{-9}
16L-Ms0.08	16Lx1L	$2048, 128^2$	0.08	0.8, 0.4, 0.28, 0.2 0.1	1.09, 1.17, 1.11, 1.10 1.11	A	[0, 4]	[3, 4]	[3, 8], [4, 9] [7, 12], [7, 12] [9, 14]	2.1×10^{-9}
16L-Ms0.02-A	16Lx1L	$2048, 128^2$	0.02	0.8, 0.4, 0.2, 0.1	1.08, 1.17, 1.04, 1.04	A	[0, 4]	[3, 4]	[3, 8], [4, 9] [13, 18], [15, 20]	2.1×10^{-9}
8L-Ms0.02-A	8Lx1L	$1024, 128^2$	0.02	0.8, 0.4, 0.2, 0.1	1.09, 1.17, 0.99, 1.01	A	[0, 4]	[3, 4]	[3, 8], [4, 9] [13, 18], [15, 20]	2.1×10^{-9}
4L-Ms0.02-A	4Lx1L	$512, 128^2$	0.02	0.8, 0.4, 0.2, 0.1	1.10, 1.19, 0.94, 1.01	A	[0, 4]	[3, 4]	[3, 8], [4, 9] [13, 18], [15, 20]	2.1×10^{-9}
1L-Ms0.02-A	1Lx1L	$128, 128^2$	0.02	0.8, 0.4, 0.2, 0.1	1.22, 1.19, 1.04, 1.11	A	[0, 4]	[3, 4]	[3, 8], [4, 9] [7, 12], [7, 12]	2.1×10^{-9}
8L-Ms0.02-Ab	8Lx1L	$1024, 128^2$	0.02	0.8, 0.4, 0.2, 0.1	1.07, 1.10, 1.09, 0.93	Ab	–	[4, 5]	[3, 8], [4, 9] [10, 15], [15, 20]	2.1×10^{-9}
8L-Ms0.02-I	8Lx1L	$1024, 128^2$	0.02	0.8, 0.4, 0.2, 0.1	1.07, 1.11, 1.19, 1.19	I	–	[3, 4]	[3, 8], [4, 9] [4, 9], [4, 9]	2.1×10^{-9}
16L-Ms0.02-low-A	16Lx1L	$1024, 64^2$	0.02	0.8, 0.4, 0.2, 0.14, 0.1	1.02, 1.12, 1.31, 1.43 1.44	A	[0, 4]	[3, 4]	[11, 15]	2.6×10^{-7}

[a] $[\tilde{t}_0, \tilde{t}_1]$ is the time interval used for the averages in time, in units of L/v_0.
[b] $\tilde{\nu}_3$, $\tilde{\eta}_3$ are the hyper-viscosity and hyper-resistivity in units of $L^5 v_0$.

Reconnection diffusion

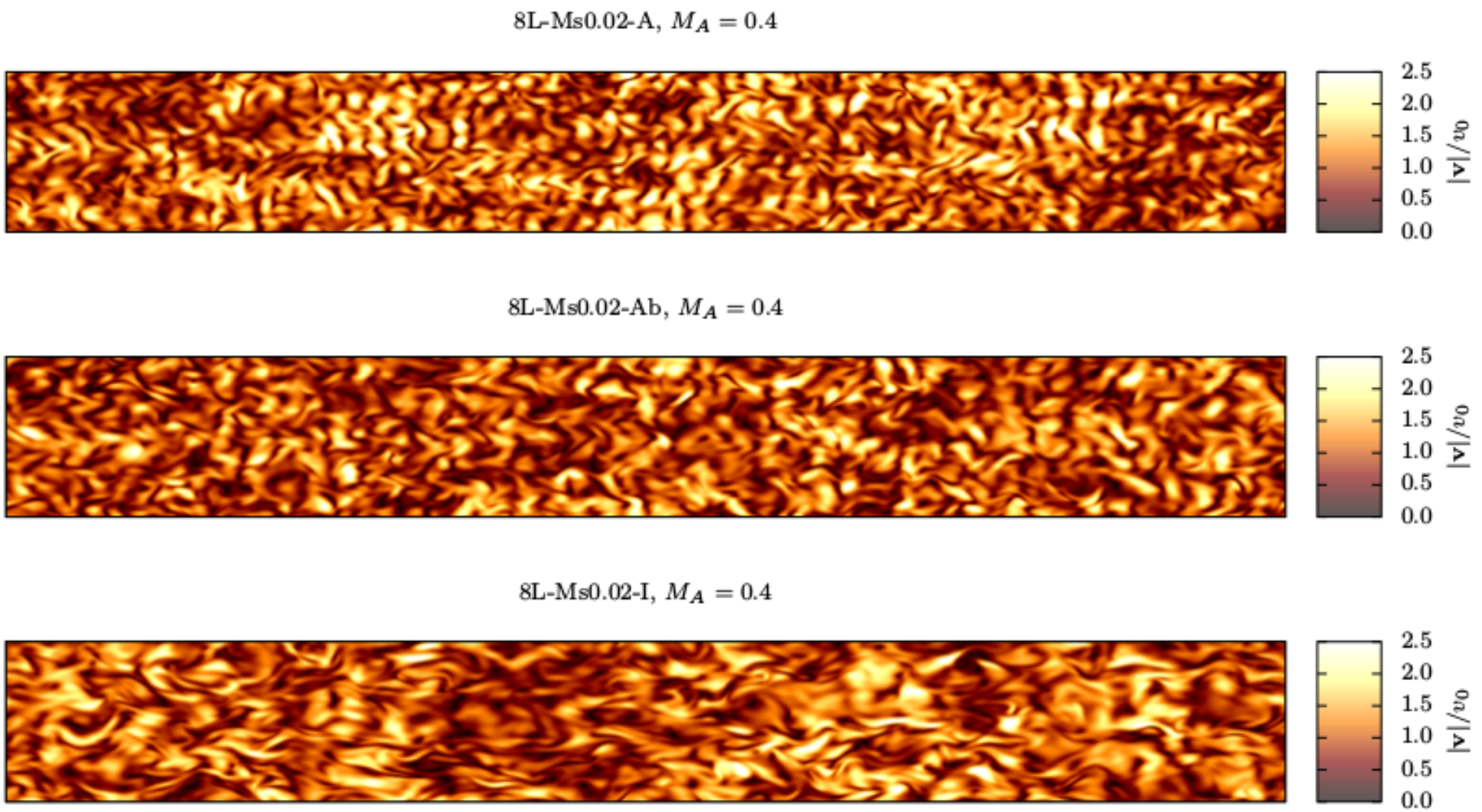

Figure 1. Central slice (xy-plane) showing the velocity modulus distribution at the final time of the simulations. Models with identical parameters but different forcing distributions in the k-space are compared. From top to bottom: A-forcing, Ab-forcing, and I-forcing. All simulations have the same Alfvénic Mach number $M_A \equiv v_0/v_{A,0} = 0.4$ and sonic Mach number $M_S = 0.02$. See Table 1 for the complete description of the simulations parameters.

Reconnection diffusion

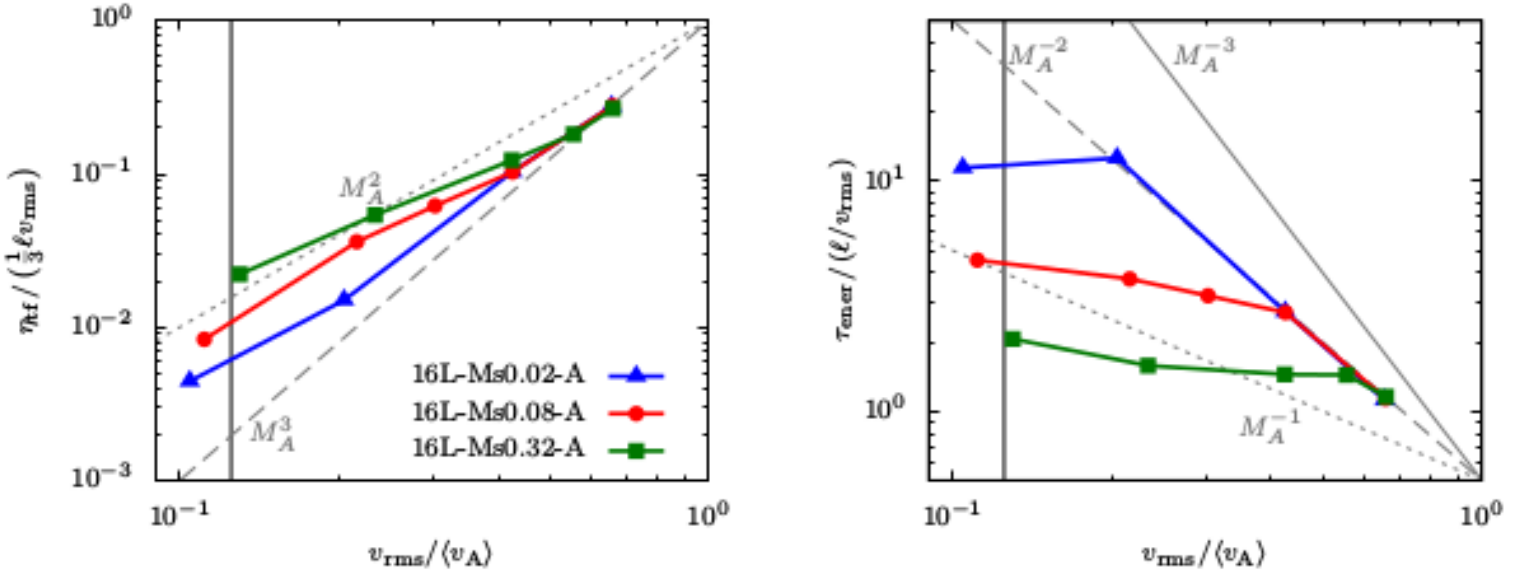

Figure 3. Magnetic diffusion coefficients $\eta_{\rm tf}$ measured by the test-field method (left) and the energy transfer time $\tau_{\rm ener} \equiv E_{\rm turb}/T_{\rm turb}$ (right), as a function of the Alfvénic Mach number $M_A = v_{\rm rms}/\langle v_A\rangle$. Simulations with the same A-forcing, the domain sizes, but different sonic Mach number $M_S = v_{\rm rms}/c_s$ are compared. Each point corresponds to one run in Table 1. For the parameters used in these simulations the vertical solid line indicates the lower limit of M_A given by Eq. 11 at the injection scale ℓ.

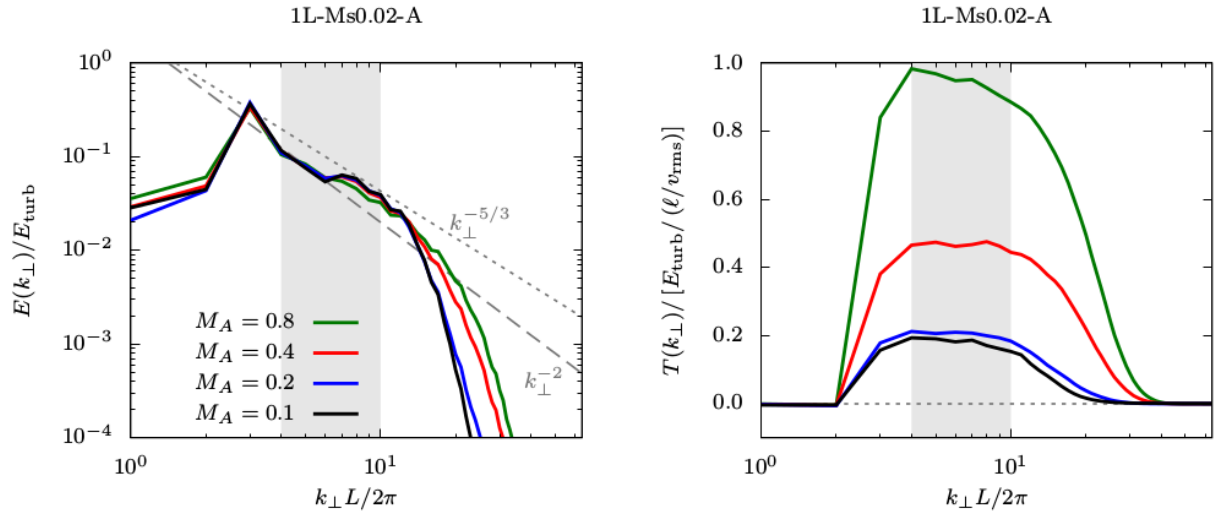

Figure 5. The energy spectrum $E(k_\perp)$ (left column) and the energy transfer spectrum $T(k_\perp)$ (right panel). In each panel, models from Table 1 with different Alfvénic Mach numbers M_A are represented by curves with different colors. Top: models with sonic Mach number $M_S = 0.32$ and domain size 16Lx1L; middle: models with $M_S = 0.02$ and domain size 16Lx1L; bottom: models with $M_S = 0.02$ and domain size 1Lx1L. The power laws $\propto k_\perp^{-5/3}$ and $\propto k^{-2}$ are also depicted for comparison in the left panels. The gray area covers the wavenumbers range $4 < k_\perp L/2\pi < 10$ for which the transfer spectrum is approximately constant and close to its maximum value.

Reconnection diffusion

The RD theory assumes that the inertial range scale laws of the weak turbulence theory can be extended to the injection scales, leading to a diffusion coefficient η proportional to the hydrodynamical value multiplied by the third power of M_A, when $M_A < 1$. We found no clear evidence of the development of the weak turbulence regime in our numerical simulations. In particular, the cascading time $\propto M_A^{-1}$ from the weak turbulence theory at the injection scale is not observed in any of our model sets. Due to limited resolution and the fast increase of the cascading time with the increase of the magnetic field intensity, our simulations do not show appreciable inertial range to allow a robust determination of the power law index of the power spectrum. Nonetheless, the diffusion coefficients we obtain seem to be consistent with the RD prediction $\eta \propto M_A^3$ when the domain size parallel to the uniform magnetic field is large enough to avoid the finite box size effects (see Nazarenko 2007 in the framework of reduced MHD) and the sonic Mach number small enough ($M_S \lesssim 0.02$). For smaller boxes and bigger values of M_S, we observed a dependence of η more consistent with M_A^2, which could be the expected dependency in the strong cascading regime.

A historic lesson: Lars Onsager on turbulence

REVIEWS OF MODERN PHYSICS, VOLUME 78, JANUARY 2006

Onsager and the theory of hydrodynamic turbulence

Gregory L. Eyink

Department of Applied Mathematics and Statistics, The Johns Hopkins University, Baltimore, Maryland 21218, USA

Katepalli R. Sreenivasan

International Center for Theoretical Physics, Trieste, Italy and Institute for Physical Science and Technology, University of Maryland, College Park, Maryland 20742, USA

(Published 17 January 2006)

Lars Onsager, a giant of twentieth-century science and the 1968 Nobel Laureate in Chemistry, made deep contributions to several areas of physics and chemistry. Perhaps less well known is his ground-breaking work and lifelong interest in the subject of hydrodynamic turbulence. He wrote two papers on the subject in the 1940s, one of them just a short abstract. Unbeknownst to Onsager, one of his major results was derived a few years earlier by A. N. Kolmogorov, but Onsager's work contains many gems and shows characteristic originality and deep understanding. His only full-length article on the subject in 1949 introduced two novel ideas—negative-temperature equilibria for two-dimensional ideal fluids and an energy-dissipation anomaly for singular Euler solutions—that

Onsager: turbulence with large Reynolds number

Review of the Onsager "Ideal Turbulence" Theory

Gregory L. Eyink[1,2]
[1] *Department of Applied Mathematics & Statistics, The Johns Hopkins University, Baltimore, MD, USA, 21218 and*
[2] *Department of Physics & Astronomy, The Johns Hopkins University, Baltimore, MD, USA, 21218*
(Dated: April 16, 2018)

In his famous undergraduate physics lectures, Richard Feynman remarked about the problem of fluid turbulence: "Nobody in physics has really been able to analyze it mathematically satisfactorily in spite of its importance to the sister sciences" [1]. This statement was already false when Feynman made it. Unbeknownst to him, Lars Onsager decades earlier had made an exact mathematical analysis of the high Reynolds-number limit of incompressible fluid turbulence, using a method that would now be described as a non-perturbative renormalization group analysis and discovering the first "conservation-law anomaly" in theoretical physics. Onsager's results were only cryptically announced in 1949 and he never published any of his detailed calculations. Onsager's analysis was finally rescued from oblivion and reproduced by this author in 1992. The ideas have subsequently been intensively developed in the mathematical PDE community, where deep connections emerged with John Nash's work on isometric embeddings. Furthermore, Onsager's method has more recently been successfully applied to new physics problems, such as compressible fluid turbulence and relativistic fluid turbulence, yielding many novel testable predictions. This note will explain Onsager's exact analysis of incompressible turbulence using modern ideas on renormalization group and conservation-law anomalies, and it will also very briefly review subsequent developments.

I. INTRODUCTION

Onsager's several contributions to the theory of turbulence have already been reviewed from a history of science point of view [2]. This note is instead intended to give a busy, working physicist a concise, accurate and painless explanation of Onsager's theory of "ideal turbulence" for a low Mach-number fluid, described by the incompressible Navier-Stokes equation

$$\partial_t \mathbf{u} + (\mathbf{u}\cdot\nabla_{\mathbf{x}})\mathbf{u} = -\nabla_{\mathbf{x}} p + \nu\triangle\mathbf{u}, \quad \nabla_{\mathbf{x}}\cdot\mathbf{u} = 0. \tag{I.1}$$

For previous physics explanations of the Onsager theory, see [3] and for an extended pedagogical presentation

the Navier-Stokes equation assume the similarity form

$$\hat{\partial}_t \hat{\mathbf{u}} + (\hat{\mathbf{u}}\cdot\hat{\nabla})\hat{\mathbf{u}} = -\hat{\nabla}\hat{p} + \frac{1}{Re}\hat{\triangle}\hat{\mathbf{u}}, \quad \hat{\nabla}\cdot\hat{\mathbf{u}} = 0 \tag{II.2}$$

with $Re = UL/\nu = 1/\hat{\nu}$ the Reynolds number. Hereafter we omit the hats $\widehat{(\cdot)}$ and understand that the limit $\nu \to 0$ is really to be interpreted as the limit $Re \to \infty$. Laboratory experiments [6, 7] and numerical simulations [8, 9] both confirm that the kinetic energy dissipation rate

$$\varepsilon(\mathbf{x}, t) := \nu|\nabla_{\mathbf{x}}\mathbf{u}(\mathbf{x}, t)|^2 \tag{II.3}$$

has space-average converging in the limit as $\nu \to 0$ and not vanishing: $\langle\varepsilon(t)\rangle \to \langle\varepsilon_\star(t)\rangle > 0$. It is furthermore

Onsager again

Magnetic stochasticity and diffusion

Amir Jafari,* Ethan Vishniac,† and Vignesh Vaikundaraman‡
Johns Hopkins University, Baltimore, USA

(Dated: August 21, 2019)

We develop a quantitative relationship between magnetic diffusion and the level of randomness, or stochasticity, of the diffusing magnetic field in a magnetized medium. A general mathematical formulation of magnetic stochasticity in turbulence has been developed in previous work in terms of the $\mathcal{L}_p$-norm $S_p(t) = \frac{1}{2}||1 - \hat{\mathbf{B}}_l.\hat{\mathbf{B}}_L||_p$, pth order magnetic stochasticity of the stochastic field $\mathbf{B}(\mathbf{x},t)$, based on the coarse-grained fields, $\mathbf{B}_l$ and $\mathbf{B}_L$, at different scales, $l \neq L$. For laminar flows, stochasticity level becomes the level of field self-entanglement or spatial complexity. In this paper, we establish a connection between magnetic stochasticity $S_p(t)$ and magnetic diffusion in magneto-hydrodynamic (MHD) turbulence and use a homogeneous, incompressible MHD simulation to test this prediction. Our results agree with the well-known fact that magnetic diffusion in turbulent media follows the super-linear Richardson dispersion scheme. This is intimately related to stochastic magnetic reconnection in which super-linear Richardson diffusion broadens the matter outflow width and accelerates the reconnection process.

I. INTRODUCTION

In the early 1940s, Onsager pointed out, but never published, the remarkable fact that the velocity field in a turbulent fluid becomes Hölder singular[1] in the limit of vanishing viscosity; $\nu \to 0$ ([1]; [2]; [3]). This approach was based on an exact mathematical analysis of the high Reynolds-number regime of incompressible hydrodynamic turbulence. Such an analysis can be called, using a slightly more modern language, a non-perturbative renormalization group analysis [2]. Both laboratory ex-

In a magnetized fluid, the magnetic diffusivity (resistivity) and viscosity may be small but finite. In the limit of vanishing magnetic diffusivity, the magnetic field seems to be frozen into the fluid. This magnetic flux-freezing principle is widely applied as an estimate to MHD equations in the laboratory and astrophysical systems with the presumption that ideal MHD holds to a good accuracy. With turbulence, ubiquitous in astrophysical and laboratory systems (see e.g., [6]; [7]; [8]; [9] and references therein), the velocity and magnetic fields become singular in the limit $\nu, \eta \to 0$ and ideal MHD

Takeaway points

-Turbulent reconnection theory matured during the last 20 years. It is still not mainstream theory of reconnection, but only an aspiring one.

-Variety of developed methods starts to be organized and divided, according to applicability in different physical situations.

-It is less and less hand-waving. Numerical simulations are becoming most important for its development, as various concepts can be tested.

-New (and old) theoretical concepts are included recently. Stay tuned.

Thank you.